

1 Reference evapotranspiration evaluation using solar radiation estimated by 2 ANN and empirical models

9 Abstract

10
11 The reference evapotranspiration (ET_o) estimation with Penman-Monteith or Priestley-
12 Taylor methods requires measurements of temperature, radiation, humidity, and wind velocity.
13 In this study, we evaluated the estimations of ET_o by Penman-Monteith (ET_o -PM) and Priestley-
14 Taylor (ET_o -PrT) methods using indirect methods of calculating solar radiation (R_s). These
15 indirect methods include the Hargreaves method, models based on Artificial Neural networks
16 (ANN) technology and models using the multi-linear regression method (MLR). Three different
17 ANN and MLR models were derived. Daily meteorological measurements from two stations in
18 northern Greece were used for the development of solar radiation models and ET_o calculation.
19 The evaluation of the indirect R_s derived models and the ET_o estimation by the two methods was
20 performed with the use of correlation coefficients (r), root mean square error (RMSE), and
21 efficiency (EF) indexes. The statistics of ET_o estimation at the two stations showed that the r and
22 EF values, between the estimated ET_o using the indirect R_s models and estimated ET_o using R_s
23 measured, were greater than 0.963 and 0.918, respectively, while the RMSE values were lower
24 than 0.646 mm d⁻¹. The statistics of R_s models, showed that the r and EF values were greater than
25 0.860 and 0.605, respectively, while the RMSE values were lower than 4.47 MJ m⁻²d⁻¹. The
26 results of ANN models in comparison to MLR models, when using the same input variables, are
27 consistent between them. These findings indicate that the Penman-Monteith and Priestley-Taylor
28 methods can accurately predict ET_o using R_s values estimated indirectly through the examined
29 methods and models.

30
31 **Keynotes:** Solar radiation; Reference evapotranspiration; Penman–Monteith method; Priestley-
32 Taylor method; Empirical methods; ANNs models; Daily datasets; Regression models.

33
34
35
36

37 1. Introduction

38 The irrigation water management, the irrigation networks planning and design, the
39 sustainability of agricultural systems, the hydrologic balance, the watershed hydrology, and the
40 droughts studies are based on the accurate estimation of the reference evapotranspiration (ET_o).

41 The ET_o estimation depend mainly upon the availability of meteorological variables. The
42 most accurate are those that are based on energy budget and the combination of radiation and
43 temperature as the Priestley-Taylor method (Priestley and Taylor, 1972), the corrected FAO-24
44 Penman method (Allen and Pruitt, 1991; Gianniou and Antonopoulos, 2007; Yao, 2009), and the
45 FAO-56 Penman-Monteith method (Allen et al., 1998).

46 The evaluation of various evapotranspiration methods includes comparison of numerous
47 equations describing evaporation or evapotranspiration. Among the articles on comparison
48 between different approaches are, among many others, the works of Xu and Singh (2002), Ampas
49 et al. (2005), Lu et al. (2005), Xystrakis and Matzarakis (2011), Rácz et al. (2013), Efthimiou et
50 al. (2013), Djaman et al. (2015), Aschonitis et al. (2015), Antonopoulos and Antonopoulos
51 (2017), Su et al. (2022).

52 The solar radiation is a meteorological variable which is either not measured or is of low
53 accuracy in many cases. Many empirical methods have been developed and evaluated to predict
54 the solar radiation using daily meteorological parameters (Despotovic et al., 2015; Zhang et al.,
55 2017; Antonopoulos et al. 2019; Zang et al. 2022; Nematchoua et al. 2022; Nawab et al. 2023).

56 During the last decades there has been a widespread interest in the application of Artificial
57 neural networks (ANNs) in the field of water sciences and specially to estimate evaporation from
58 free water surface as well as actual and reference evapotranspiration (Jain et al., 2008;
59 Diamantopoulou et al., 2011; Laaboudi et al., 2012; Heddami, 2014; Antonopoulos et al., 2016;
60 Antonopoulos et al., 2019; Nematchoua et al., 2022; Nawab et al., 2023, among others) and
61 climate variables.

62 In Antonopoulos et al. (2019), the suitability of Hargreaves method, Artificial Neural
63 networks (ANN) and multi-linear regression methods (MLR) to estimate solar radiation was
64 evaluated using daily meteorological data from two stations in Northern Greece. Daily data of
65 three successive years were used in this work. The use of extraterrestrial radiation (R_a) and the
66 square root of daily difference in temperature, $(T_{max}-T_{min})^{0.5}$, in the ANN and MLR models
67 resulted in more accurate estimations.

68 The main objective of this study is to evaluate the computed ET_o using the Penman –
69 Monteith and Priestley-Taylor methods, in which the solar radiation variable is estimated using

70 indirect methods, including models based on ANNs and MLR methods. An analytical work on
 71 derivation of indirect methods suitability was presented in Antonopoulos et al (2019). The R_s and
 72 ET_o of Hargreaves method is also evaluated. The indirect R_s models and the results of ET_o were
 73 derived and evaluated using daily data at two meteorological stations. The daily datasets covered
 74 five consecutive years at these two meteorological stations located in northern Greece, areas of
 75 high significance in agricultural irrigation and water resources management.

76

77 2. Materials and methods

78 2.1 Daily reference crop evapotranspiration

79 The FAO-56 Penman-Monteith (PM) method of daily reference crop evapotranspiration
 80 (ET_o -PM), which consider according to FAO the standard method, is described by the following
 81 equation (Allen et al. 1998):

$$82 \quad ET_o = \frac{0.408\Delta(R_n - G) + \gamma \frac{900}{T + 273} u_2 (e_a - e_d)}{\Delta + \gamma(1 + 0.34u_2)} \quad (1)$$

83 where ET_o is the daily reference crop evapotranspiration (mm d^{-1}), R_n is the net radiation ($\text{MJ m}^{-2}\text{d}^{-1}$),
 84 u_2 is the mean wind speed at 2 m above soil surface (m s^{-1}), T is the mean air temperature
 85 ($^{\circ}\text{C}$), G is the soil heat flux density at the soil surface ($\text{MJ m}^{-2}\text{d}^{-1}$), e_a is the saturation vapour
 86 pressure (kPa), e_d is the actual vapour pressure (kPa), Δ is the slope of the saturation vapour
 87 pressure-temperature curve ($\text{kPa}^{\circ}\text{C}^{-1}$), γ is the psychrometric constant ($\text{kPa}^{\circ}\text{C}^{-1}$).

88 The Priestley-Taylor method (Priestley and Taylor, 1972) of daily reference crop
 89 evapotranspiration (ET_o -PrT) is a modification and simplification of the Penman formula. It
 90 described by the following form:

$$91 \quad ET_o = \alpha \frac{\Delta}{\Delta + \gamma} \frac{(R_n - G)}{\rho_w \lambda} \quad (2)$$

92 where λ is the latent heat of vaporization (MJ kg^{-1}), ρ_w is the water density (kg m^{-3}) and α is an
 93 empirically derived parameter with an average value of 1.26 (Sene et al. 1991, Aschonitis et al.,
 94 2015). This method is a radiation based method. The Priestley-Taylor method has been used to
 95 estimate the reference crop evapotranspiration in many works (Utset et al., 2004; Bogawski and
 96 Bednorz, 2014; Aschonitis et al., 2015; Antonopoulos et al, 2017).

97 The Hargreaves method (Hargreaves and Samani, 1985) estimates daily ET_o , with the
 98 following equation

$$99 \quad ET_o = (a_h / K_{RS}) (T_{\text{mean}} + b_h) R_s \quad (3)$$

100 where T_{mean} is the mean temperature ($^{\circ}\text{C}$), and $a_h=0.0023 \text{ }^{\circ}\text{C}^{-1.5}$, and $b_h=17.8 \text{ }^{\circ}\text{C}$ empirical
 101 constants, K_{RS} is the adjustment coefficient of the radiation formula ($^{\circ}\text{C}^{-0.5}$), and R_s is the solar
 102 radiation (mm d^{-1}) of Hargreaves equation.

103 The incoming shortwave solar radiation R_s ($\text{MJ m}^{-2} \text{ d}^{-1}$), according to Hargreaves and
 104 Samani (1982; 1985), is computed by the following equation:

$$105 \quad R_s = K_{RS} \cdot R_a \cdot (TD)^{0.5} \quad (4)$$

106 where R_a is the extraterrestrial radiation ($\text{MJ m}^{-2} \text{ d}^{-1}$) and TD (equal to $T_{\text{max}}-T_{\text{min}}$) is the
 107 temperature difference between maximum (T_{max}) and minimum (T_{min}) daily temperature ($^{\circ}\text{C}$).
 108 Hargreaves (1994) recommended using $K_{RS}= 0.162$ for “interior” locations, and $K_{RS} = 0.19$ for
 109 coastal locations. (Daut et al., 2011; Raziei and Pereira, 2013; Antonopoulos and Antonopoulos,
 110 2017; Rivero et al., 2017; Aschonitis et al. 2017).

111 The Multivariable regression method (MLR) is based on the fact that the meteorological
 112 parameters are highly correlated with R_s and ET_o . A general form of these equations is as

$$113 \quad R_s = m_1 + m_2X_1 + m_3X_2 + m_4X_3 + \dots + m_{n+1}X_n \quad (5)$$

114 where m_1, m_2, m_3, m_4 and m_n are regression coefficients and X_i are meteorological parameters or
 115 factors. The variables of X_i can be simple meteorological parameters ($T_{\text{ave}}, T_{\text{max}}, T_{\text{min}}, RH_{\text{av}}, u_2$)
 116 or combinations of them ($(TD=T_{\text{max}}-T_{\text{min}})$ and $(TD)^{0.5}$) (Alexandris et al., 2006; El-Sebaai et al.,
 117 2010; Li et al., 2011; Besharat et al., 2013; Valiantzas, 2018).

118

119 **2.3. Artificial neural networks**

120 The artificial neural networks are non-linear models that make use of a structure capable
 121 to represent arbitrary complex non-linear processes that relate the inputs and outputs of any
 122 system (Jain et al., 2008; Diamantopoulou et al., 2011; Laaboudi et al., 2012; Yadav and Chandel,
 123 2014; Kumar et al. 2011; Kisi et al, 2015; Premalatha and Valan Arasu, 2016; Antonopoulos et
 124 al., 2016; Zhang et al., 2017; Antonopoulos and Antonopoulos, 2017).

125 In this article, an algorithm of the multi-layer feed forward artificial neural networks and
 126 of the back-propagation for optimization was used (Premalatha and Vala Arasu, 2016). The main
 127 task in developing an ANN model is to identify the input variables and the optimal network
 128 structure in order to produce the desired output accurately. Before training and testing, the
 129 variables (as example $T_{\text{max}}, T_{\text{min}}, T_{\text{av}}, RH_{\text{av}}, u_2$) were standardized and were used as input
 130 variables. The target output variable (as R_s) was also standardized before training and testing.

131 The trial and error procedure showed that the number of neurons in the hidden layer is
 132 between 4 and 6, because they are produced similar results. Details of ANN models selection and
 133 the procedure that followed in this study have been presented elsewhere (Jain et al., 2008;
 134 Antonopoulos et al. 2016); Antonopoulos and Antonopoulos 2017).

135

136 2.4. Modeling Performance Criteria

137 The model's performance was evaluated using statistical criteria including the correlation
 138 coefficient (r), the root mean square error (RMSE) and the coefficient of efficiency (EF):

$$139 \quad r = \left(\frac{\sum_{i=1}^N (O_i - O_m)(C_i - C_m)}{\sqrt{\sum_{i=1}^N (O_i - O_m)^2} \sqrt{\sum_{i=1}^N (C_i - C_m)^2}} \right) \quad (6)$$

$$140 \quad \text{RMSE} = \sqrt{\frac{1}{N} \sum_{i=1}^N (C_i - O_i)^2} \quad (7)$$

$$141 \quad \text{EF} = 1 - \left(\frac{\sum_{i=1}^N (C_i - O_i)^2}{\sum_{i=1}^N (O_i - O_m)^2} \right) \quad (8)$$

142 where O are the observed values (the solar radiation or the reference evapotranspiration), C are
 143 the computed values by the other methods and O_m and C_m are the mean observed and computed
 144 values, respectively. In most cases the coefficient of determination (R^2) is the square of r . The
 145 range of EF (which is also known as Nash and Sutcliffe model efficiency) lies between 1 (perfect
 146 value) and $-\infty$.

147

148 2.5. Study area and data

149 The meteorological data, that was used in this study to estimate daily solar radiation and
 150 ET_o , are consisted of daily data of air temperature, solar radiation, wind speed, and humidity for
 151 a period of five years (2011 to 2015) measured at two meteorological station in northern Greece
 152 (Antonopoulos et al. 2019).

153 The 1st meteorological station of Aristotle University of Thessaloniki Farm (AUTH) is
 154 located in Central Macedonia (40° 37'54''N, 22° 57'27''E, 34 m above sea level) and the 2nd
 155 meteorological station of Amyntaio (AMIN) at West Macedonia is located at northern latitude
 156 of 40° 46'27''N, 21°39'E, 580 m above sea level.

157 Table 1 presents the average and standard deviation values of temperature (°C), relative
 158 humidity (%), wind velocity (m s^{-1}), and solar radiation ($\text{MJ m}^{-2} \text{d}^{-1}$) for each station for the study
 159 period of five years. The daily data sets of meteorological station of AUTH present missing data
 160 which estimated to 17 % of available data.

161

162 *Table 1. Average temperature, relative humidity, wind velocity and solar radiation for each station*
 163 *during study period*

	T, oC		RH, %		u ₂ , m sec ⁻¹		R _s , MJ m ⁻² d ⁻¹	
	mean	sd	mean	sd	mean	sd	mean	sd
AUTH	16.43	8.23	70.57	15.48	0.56	0.80	15.94	8.58
AMIN	12.59	8.56	66.07	15.16	1.80	1.14	17.19	9.29

164

165

166 3. RESULTS

167

168 The results of Hargreaves equation, ANNs and MLR models to estimate the R_s are
 169 presented firstly in this part of article. Meteorological data sets of 3 years, from the same station,
 170 were used in a former published paper (Antonopoulos et al., 2019) to evaluate the R_s models. In
 171 the present study 5 years of daily data are employed. Therefore, only the more important
 172 information are showcased here.

173 Subsequently, this section examines mainly the impact of employing the indirectly
 174 estimated R_s (via empirical and ANN models) as inputs for ET_o calculations using the Penman-
 175 Monteith, the Priestley-Taylor and Hargreaves equations.

176

177 3.1. Results of estimated R_s at Aristotle University Farm Station

178 The daily datasets of 5 years at Aristotle University Farm station was used to derive the
 179 Hargreaves (HG) equation of R_s estimation. The daily R_s values predicted by the Hargreaves
 180 (HG) method using the recommended value of K_{RS} coefficient (K_{RS}=0.162) and the value adjusted
 181 to local conditions (K_{RS}=0.158), compared with the R_s measurements. In Table 2 the values of
 182 statistical criteria of these comparisons are presented. The correlation coefficient (r), the RMSE
 183 and EF of the Hargreaves method for R_s are 0.893, 3.049 MJ m⁻²d⁻¹ and 0.732, respectively for
 184 K_{RS}=0.162, and 0.893, 3.032 MJ m⁻²d⁻¹ and 0.722, respectively for K_{RS}=0.158.

185 The architecture of the ANN model was identified by the trial and error procedure
 186 (Antonopoulos and Antonopoulos, 2017; Antonopoulos et al. 2019). Three different ANN
 187 models were developed. The difference, among them, are in the number and the combination of
 188 input variables. The input and output variables were standardized before training and testing.

189 In the 1st model, the standard meteorological parameters (T_{max}, T_{min}, T_{ave}, RH_{av}, u₂) were used
 190 as input variables. The most appropriate architecture of this model (ANN-I), that finally chosen,
 191 was the 5-6-1 structure, with 5 neurons in the input layer, 6 neurons in the hidden layer and 1

192 neuron in the output layer which corresponds to the solar radiation. All of the available data sets
 193 were used for training and testing the model.

194 Two other cases of input variables were examined. In one of them (ANN-II), four (4) input
 195 variables were used [R_a , $(T_{max}-T_{min})$, $(T_{max}-T_{min})^{0.5}$, RH_{av}], while in the other (ANN-III), two (2)
 196 variables, the R_a , and $(T_{max}-T_{min})^{0.5}$ were used.

197 In Table 2 the statistical properties of three different ANNs models to estimate R_s at
 198 Aristotle University Farm station are presented. The correlation coefficient (r), the RMSE and
 199 EF of the ANNs models for R_s ranged from 0.861 to 0.925, the RMSE ranged from 3.271 to
 200 4.451 MJ m²d⁻¹ and the EF ranged from 0.652 to 0.806.

201 The derived MLR equations, which are based on the available variables of the daily datasets
 202 of 2011-15 and different combinations of independent variables, are given as

203
 204 $R_s = 8.6705 + 0.2407T_{max} - 1.2386T_{min} + 1.4692T_{ave} - 0.1299RH_{av} + 0.1466u_2$ (8)

205 $R_s = -4.4342 + 0.4355R_a - 0.2949(T_{max} - T_{min}) + 5.8188(T_{max} - T_{min})^{0.5} -$
 206 $0.13702RH_{av}$ (9)

207 $R_s = -17.6084 + 0.5367R_a + 5.2621(T_{max} - T_{min})^{0.5}$ (10)

208 The r² of these approaches are 0.758, 0.811 and 0.850, respectively.

209 In Table 2 the statistical properties of three different MLRs models to estimate R_s at
 210 Aristotle University Farm station are presented. The correlation coefficient (r) of the MLRs
 211 models for R_s ranged from 0.871 to 0.922, the RMSE ranged from 3.502 to 4.178 MJ m²d⁻¹ and
 212 the EF ranged from 0.681 to 0.780.

213 *Table 2.*

214 *Statistical criteria of ANN model to estimate R_s at Aristotle University Farm station*

	R_s		index			Ranking		
	Average MJ m ² d ⁻¹	sd MJ m ² d ⁻¹	r	RMSE MJ m ² d ⁻¹	EF	r	RMSE	EF
Measured	15.940							
HG	16.441	7.506	0.893	3.049	0.732	4	2	5
HG local	16.035	7.320	0.893	3.032	0.722	4	1	6
ANN -I	14.906	7.551	0.861	4.451	0.652	6	8	8
ANN -II	16.300	7.436	0.925	3.271	0.806	1	3	1
ANN -III	15.713	7.669	0.893	3.837	0.750	4	6	4
MLR -I	15.938	7.404	0.871	4.178	0.681	5	7	7
MLR -II	15.936	7.655	0.900	3.697	0.767	3	5	3
MLR -III	14.805	7.472	0.922	3.502	0.780	2	4	2

215 Note:

216 ANN-I (T_{max} , T_{min} , T_{ave} , RH_{av} , u_2); ANN -II { R_a , $(T_{max}-T_{min})$, $(T_{max}-T_{min})^{0.5}$, RH_{av} }; ANN -III{ R_a , $(T_{max}-T_{min})^{0.5}$ }
 217 MLR -I (T_{max} , T_{min} , T_{ave} , RH_{av} , u_2); MLR -II { R_a , $(T_{max}-T_{min})$, $(T_{max}-T_{min})^{0.5}$, RH_{av} }; MLR -III{ R_a , $(T_{max}-T_{min})^{0.5}$ }

218

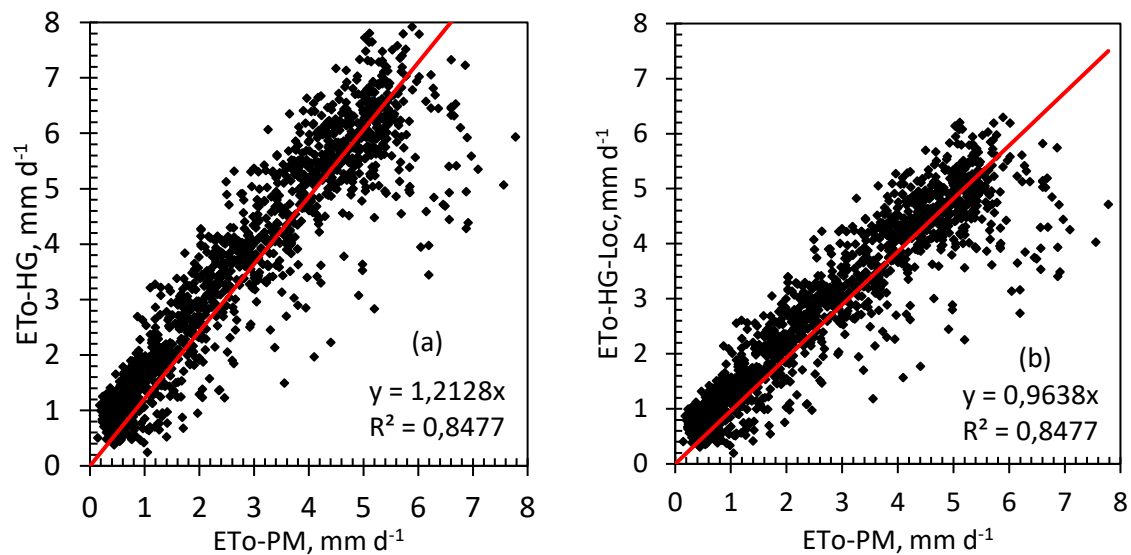
219 The estimated values of R_s using MLR-III and ANN-II models correlated very well with
 220 the measured values of R_s , outperforming other MLR and ANN models as well as the Hargreaves
 221 method. The ANN-I and MLR-I showed lower accuracy.

222

223 3.2 Results of ET_o at Aristotle University Farm Station

224 Figure 1 shows the comparison of daily ET_o values estimated using the R_s values of
 225 Hargreaves equations (original and modified to local conditions) and the ET_o values estimated
 226 by Penman – Monteith method using the measured values of R_s at Aristotle University Farm
 227 station.

228

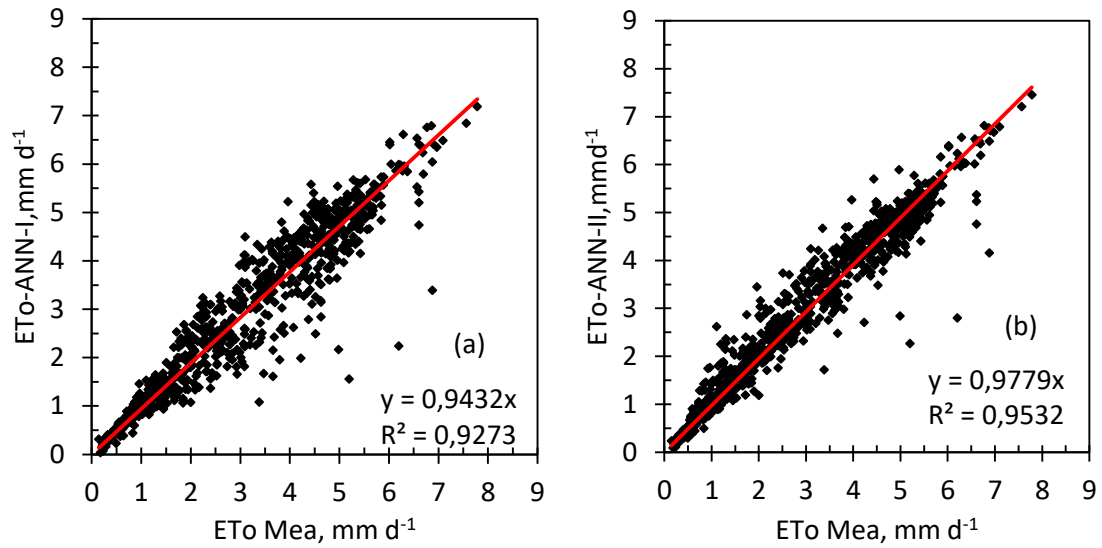


229

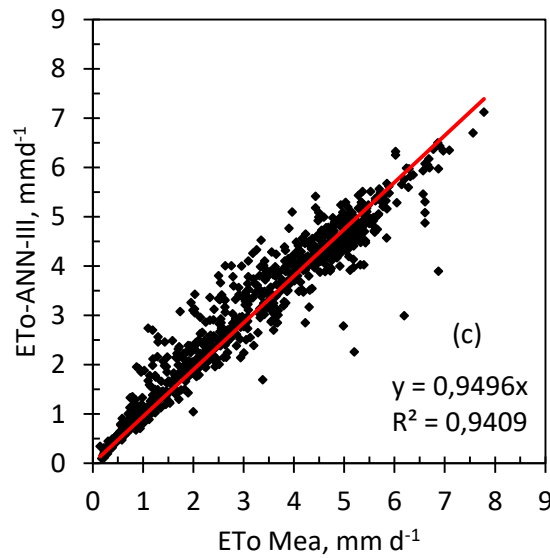
230 *Figure 1. Scattering diagrams of daily ET_o estimated by the Hargreaves (HG) and the ET_o values*
 231 *estimated by the Penman – Monteith method using measured values of R_s , a) $K_{RS}=0.162$; b) $K_{RS}=0.158$*
 232 *local adjusted coefficient.*

233

234 Figures 2 presents the scattering diagrams between ET_o of Penman-Monteith method using
 235 R_s estimated using the ANN models and the measured values of R_s at Aristotle University Farm,
 236 respectively.



237



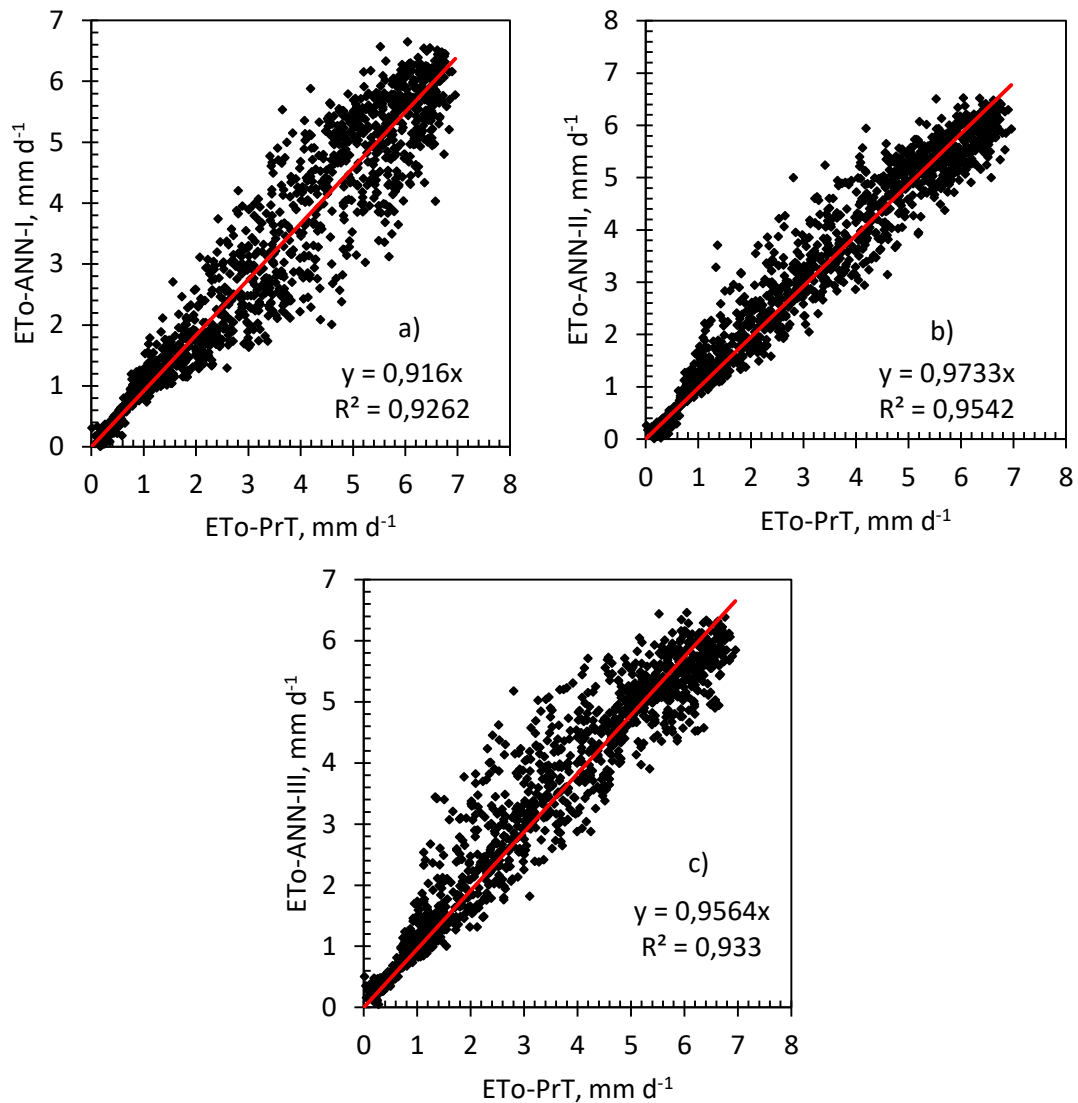
238

239 *Figure 2. Scattering diagrams between ET_o estimated with R_s measured and ET_o estimated with R_s*
 240 *computed with Artificial Neural Networks (a. ANN-I; b. ANN-II and c. ANN-III) models at Aristotle*
 241 *University Farm station.*

242

243 Figures 3 presents the scattering diagrams between ET_o of Priestley-Taylor method using R_s
 244 estimated using the ANNs models and the measured values of R_s at Aristotle University Farm,
 245 respectively.

246



247

248

249 *Figure 3. Scattering diagrams of ET_0 -PrT estimated with R_s measured and ET_0 -PrT estimated with R_s*
 250 *computed with Artificial Neural Networks (a. ANN-I; b. ANN-II and c. ANN-III) models at Aristotle*
 251 *University Farm station.*

252

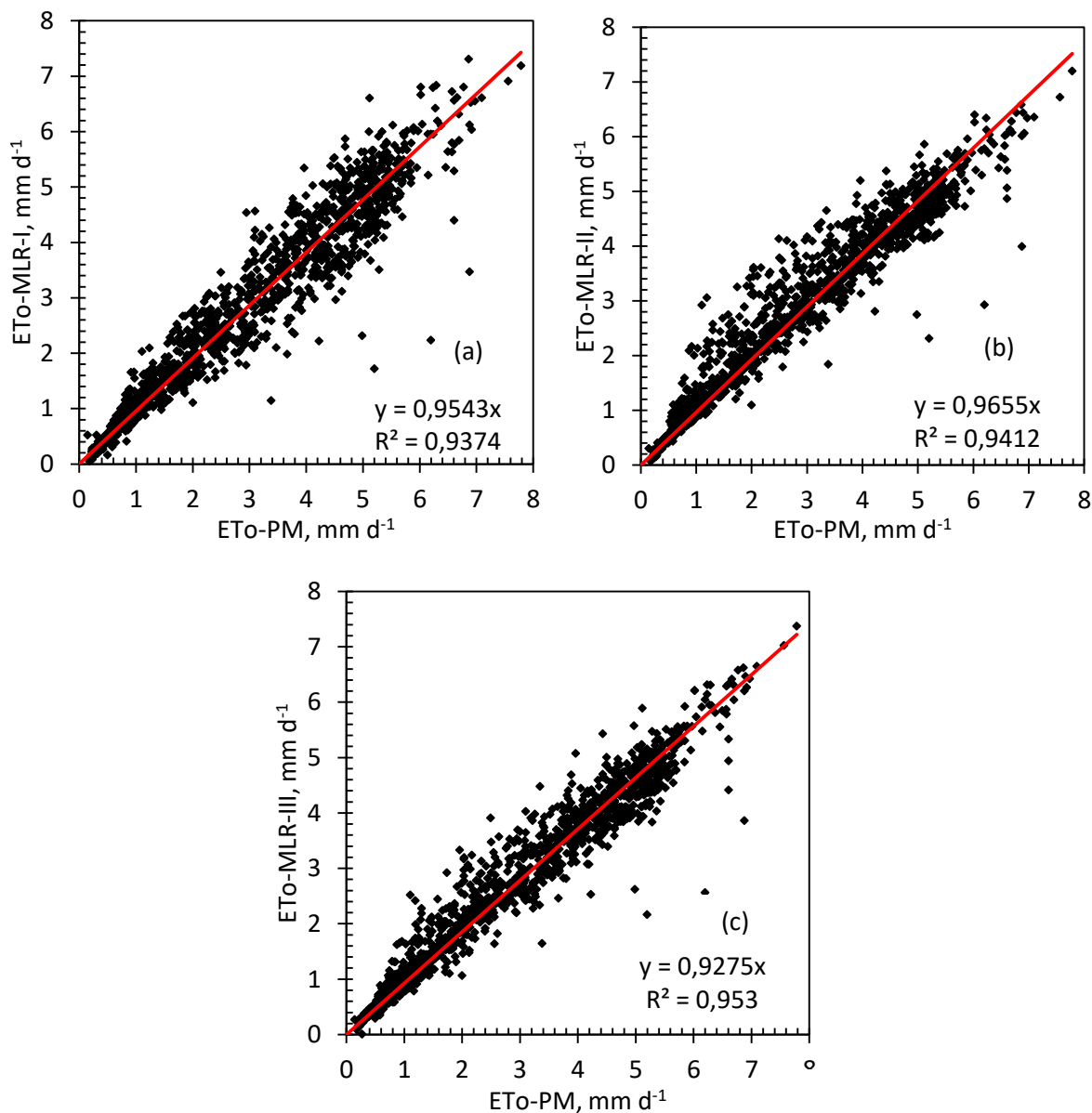
253 The values of R^2 are very high in these three scatters diagrams (0.926 to 0.954).

254 Underestimation of higher values of ET_0 -PrT observed, with lower using the ANN-I model.

255 Figures 4 presents the comparison between ET_0 of Penman-Monteith method using R_s

256 estimated using the MLR models and the measured values of R_s at Aristotle University Farm,

257 respectively.



258

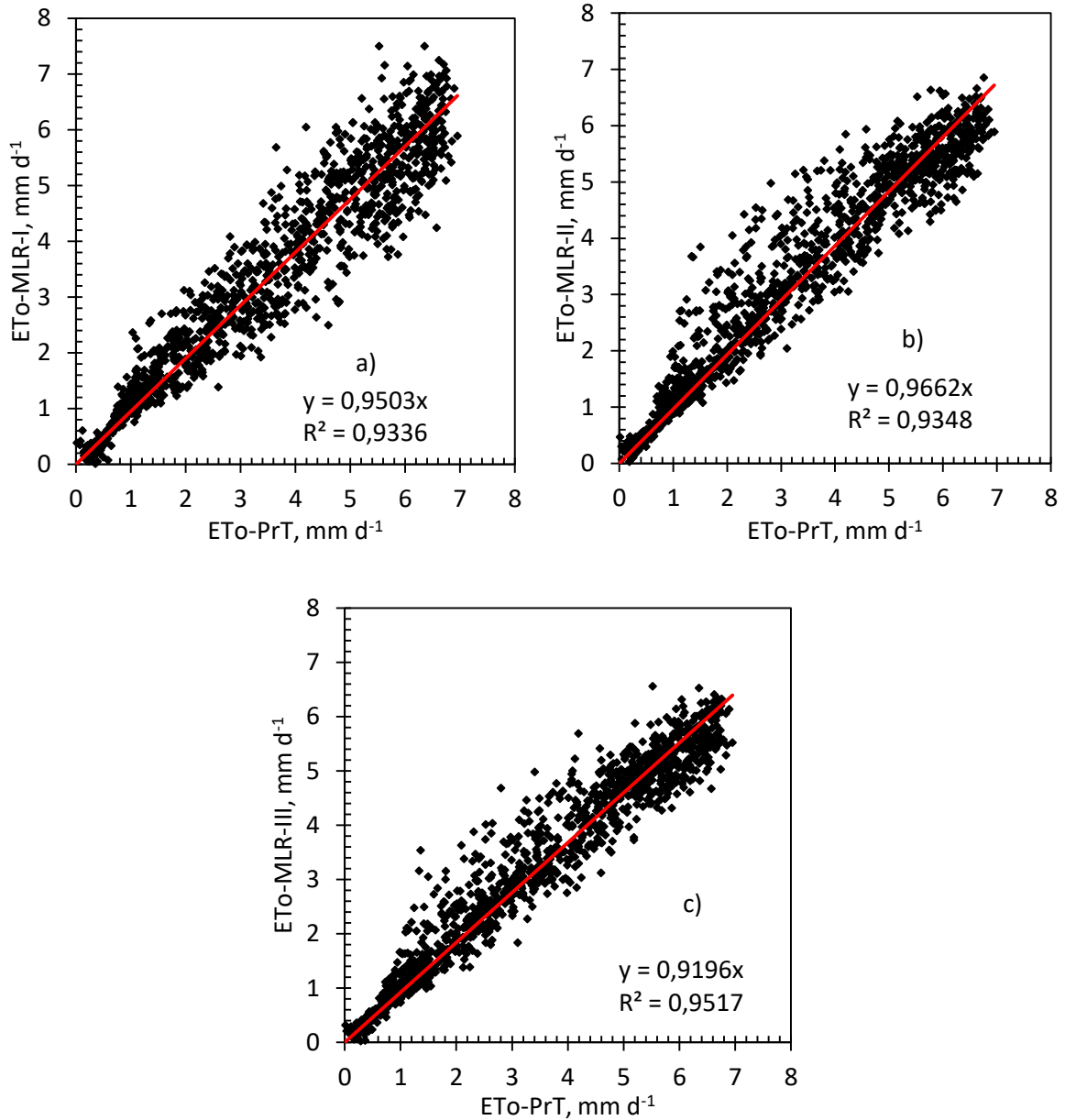
259

260

261 *Figure 4. Scattering diagrams between ET_o estimated with R_s measured and ET_o estimated with R_s*
 262 *computed with Multi linear regression (a. MLR-I, b. MLR-II and c. MLR-III) models at Aristotle*
 263 *University Farm station.*

264

265 Figures 5 presents the comparison between ET_o of Priestley-Taylor method using R_s
 266 estimated using the MLR models and the measured values of R_s at Aristotle University Farm,
 267 respectively.



268

269

270

271

272

273

274

275

276

277

278

279

280

281

Figure 5. Scattering diagrams of ET₀-PrT estimated with R_s measured and ET₀-PrT estimated with R_s computed with Multi linear regression (a. MLR-I, b. MLR-II and c. MLR-III) models at Aristotle University Farm station.

The values of R² are very high in these three scatters diagrams (0.933 to 0.951). Underestimation of higher values of ET₀-PrT is also observed, with lower values when the MLR-III model is used.

Table 3 presents the statistical properties of different methods to estimate ET₀, using the indirect methods of R_s estimation.

The correlation coefficient of the Hargreaves method for ET₀ is 0.932 using both approaches of R_s.

282 The r of ANNs models ranged from 0.910 to 0.978, and of MLR, it ranged from 0.963 to
 283 0.988 for ET_o-PM method, while it ranged from 0.984 to 0.991 for ANNs and from 0.986 to
 284 0.990 for MLR of ET_o-PrT method. The MLR models correlated very well with the measured
 285 values of ET_o, followed by the ANN models and Hargreaves method.

286 The scattering diagrams and the comparison between the estimated values of ET_o, along
 287 with the statistical criteria, show that the evaluated ET_o with the Penman-Monteith and Priestley-
 288 Taylor methods, while using indirect methods to estimate the R_s, is highly correlated with the
 289 values of ET_o estimated with measurements of R_s.

290
 291 *Table 3.*

292 *Statistical criteria of ET_o of PM and PrT methods estimation at Aristotle University Farm station using*
 293 *the indirect method of R_s computing.*

	ET _o -PM				ET _o -PrT			
	Ave mm d ⁻¹	r	RMSE mm d ⁻¹	EF	ave mm d ⁻¹	r	RMSE mm d ⁻¹	EF
ANN -I	2.413	0.963	0.410	0.917	2.72	0.984	0.626	0.960
ANN -II	2.566	0.978	0.314	0.952	2.93	0.991	0.450	0.982
ANN -III	2.550	0.973	0.356	0.932	2.90	0.987	0.541	0.972
MLR -I	2.736	0.983	0.371	0.965	2.84	0.986	0.558	0.971
MLR -II	2.788	0.988	0.313	0.975	2.93	0.987	0.529	0.974
MLR -III	2.800	0.985	0.355	0.968	2.78	0.990	0.529	0.971
HG	3.358	0.932	0.889	0.712				
HG local	2.669	0.932	0.693	0.826				

294

295

296 **3.3. R_s model derivation at Amyntaio Station**

297 The statistical properties of the methods used to estimate R_s at Amyntaio meteorological
 298 station are presented in Table 4. More details and scatter diagrams slightly different were
 299 presented at Antonopoulos et al. (2019). The value of K_{RS} coefficient adjusted to local conditions
 300 is K_{RS}=0.178. The correlation coefficient (r), the RMSE and EF of the Hargreaves method for R_s
 301 are 0.908, 4.197 MJ m⁻²d⁻¹ and 0.688, respectively for K_{RS}=0.162, and 0.908, 3.857 and 0.782,
 302 respectively for K_{RS}=0.178.

303 The same procedure was followed to select the ANN models with the daily data sets of
 304 Amyntaio station, three different models was examined. The input variables for the 1st ANN-I
 305 model (ANN 5-6-1) are T_{max}, T_{min}, T_{ave}, RH_{av}, u₂, while in the 2nd ANN-II (ANN 4-6-1) are R_a,
 306 (T_{max}-T_{min}), (T_{max}-T_{min})^{0.5} and RH_{av}, and in the 3rd ANN-III (ANN 2-6-1) model the input
 307 variables are R_a, and (T_{max}-T_{min})^{0.5}. In Table 4 the statistical properties of three different ANNs
 308 models to estimate R_s at Amyntaio station are presented. The correlation coefficient (r) of the

309 ANNs models for R_s ranged from 0.890 to 0.936, the RMSE ranged from 3.274 to 4.202 MJ m⁻²d⁻¹
 310 and the EF ranged from 0.734 to 0.848.

311 The MLR equations, which is based on the available variables of the daily datasets of 2011
 312 to 2015 at Amyntaio station, are given as

313 $R_s = 16.1099 + 0.4415T_{max} - 0.5583T_{min} - 0.6654T_{ave} - 0.2045RH_{av} + 0.7657u_2$ (11)

314 $R_s = 4.0126 + 0.4811R_a - 0.0478(T_{max} - T_{min}) + 3.7292(T_{max} - T_{min})^{0.5} - 0.1862RH_{av}$ (12)

315 $R_s = -15.9673 + 0.5696R_a + 5.1011(T_{max} - T_{min})^{0.5}$ (13)

316 The R² of these approaches are 0.789, 0.862 and 0.807, respectively. In Table 4 the statistical
 317 properties of three different MLRs models to estimate R_s at Amyntaio station are presented. The
 318 correlation coefficient (r) of the MLR models for R_s ranged from 0.889 to 0.929, the RMSE
 319 ranged from 3.408 to 4.210 MJ m⁻²d⁻¹ and the EF ranged from 0.734 to 0.840.

320 The values of R_s computed with the ANN-II model correlate better with the measured
 321 values of R_s , followed by the MLR-II model. The other ANN and MLR models, as well as the
 322 Hargreaves method, show lower accuracy.

323

324

Table 4.

325

Statistical criteria of Hargreaves, ANN and MLR models to estimate R_s at AMYNTAIO station

	R_s		index			ranking		
	Average MJ m ⁻² d ⁻¹	sd MJ m ⁻² d ⁻¹	r	RMSE MJ m ⁻² d ⁻¹	EF	r	RMSE	EF
Measured	16.899	9.187						
HG	15.457	7.515	0.908	4.197	0.688	4	6	7
HG Local	16.984	8.257	0.908	3.857	0.782	4	4	4
ANN-I	16.629	8.151	0.890	4.202	0.734	6	7	6
ANN-II	16.480	8.409	0.936	3.274	0.848	1	1	1
ANN-III	16.936	8.327	0.909	3.837	0.788	3	3	3
MLR-I	16.891	8.171	0.889	4.210	0.734	7	8	6
MLR-II	16.899	8.531	0.929	3.408	0.840	2	2	2
MLR-III	16.899	8.254	0.898	4.032	0.761	5	5	5

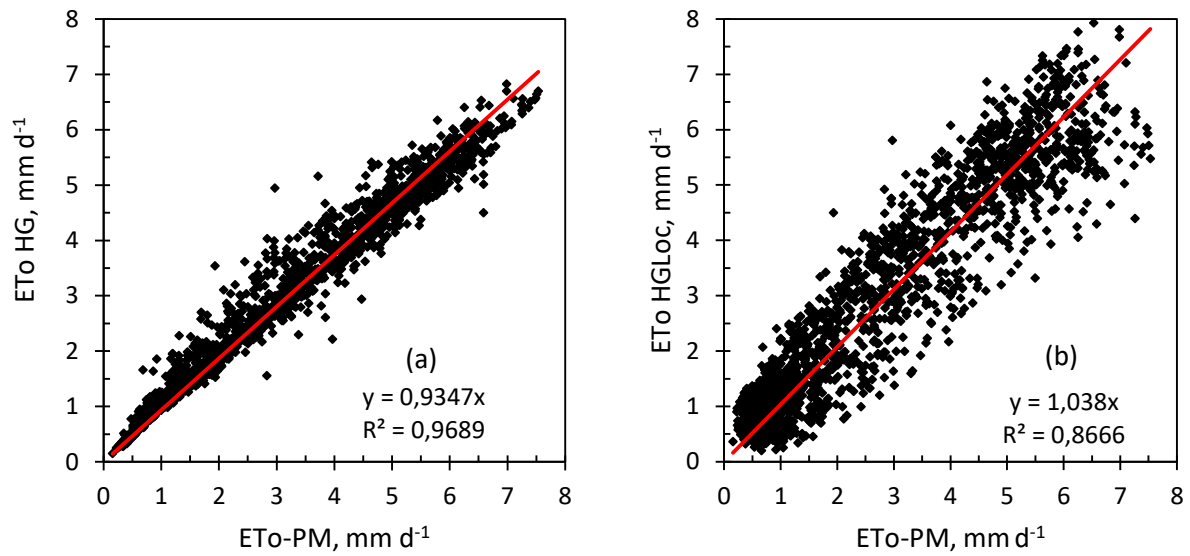
326

327

328 **3.4 Results of ET_o at Amyntaio Station**

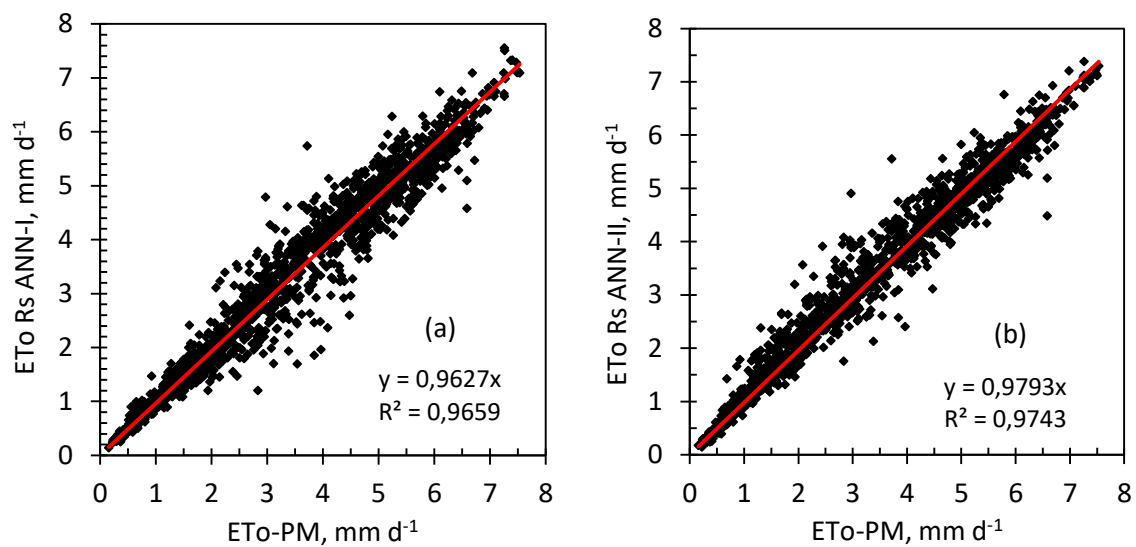
329

330 Figure 6 shows the comparison of daily ET_o values estimated using the R_s values of
 331 Hargreaves equations (original and modified to local conditions) and the ET_o estimated by
 332 Penman –Monteith method using the measured values of R_s at Amyntaio Station.

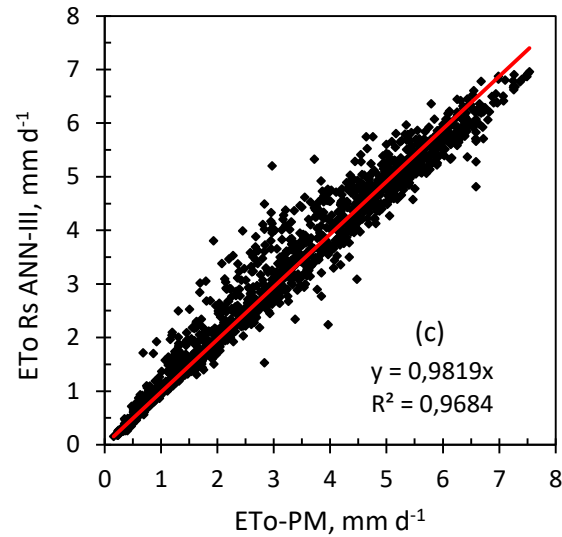


333
 334 *Figure 6. Scattering diagrams between ET_o estimated with Hargreaves (HG) method (a. original and b.*
 335 *local adjustment) against the ET_o of Penman-Monteith method using R_s measured values at Amyntaio*
 336 *Station.*

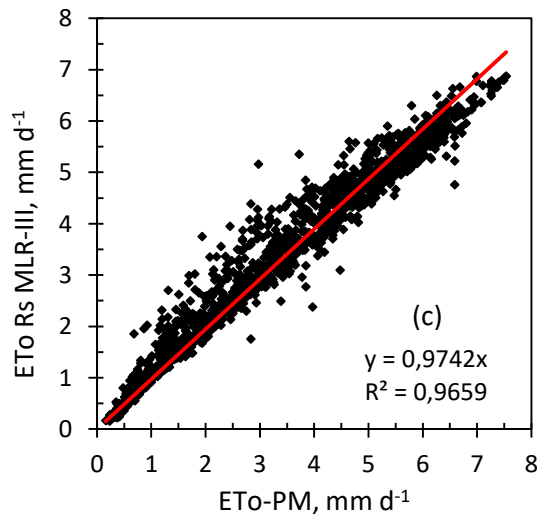
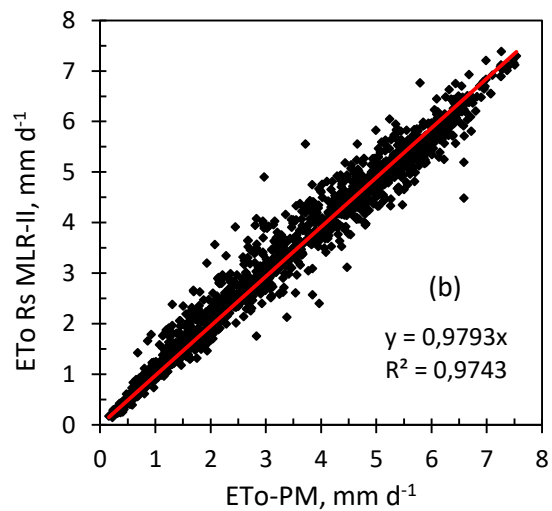
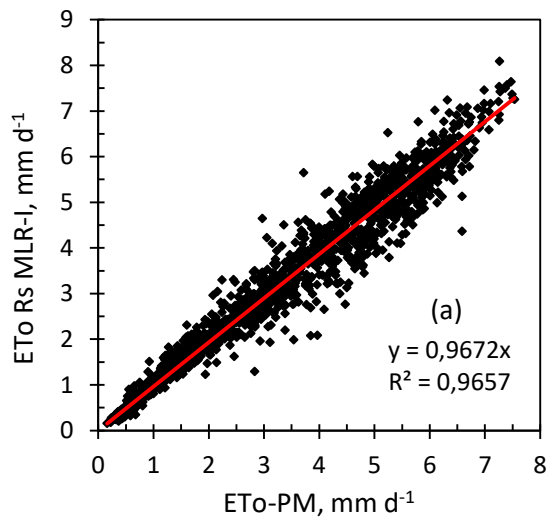
337
 338 Figures 7 and 8 present the comparison between ET_o -PM estimated using R_s measurements
 339 and ET_o -PM estimated with R_s computed with a) Artificial Neural Networks (ANNs) and b)
 340 multilinear regression (MLR) models at Amyntaio Station.



341



342
 343 *Figure 7. Scattering diagrams between ET_o -PM estimated with R_s measured and ET_o -PM estimated with*
 344 *R_s computed with Artificial Neural Networks (a. ANN-I, b. ANN-II and c. ANN-III) models at Amyntaio*
 345 *station.*

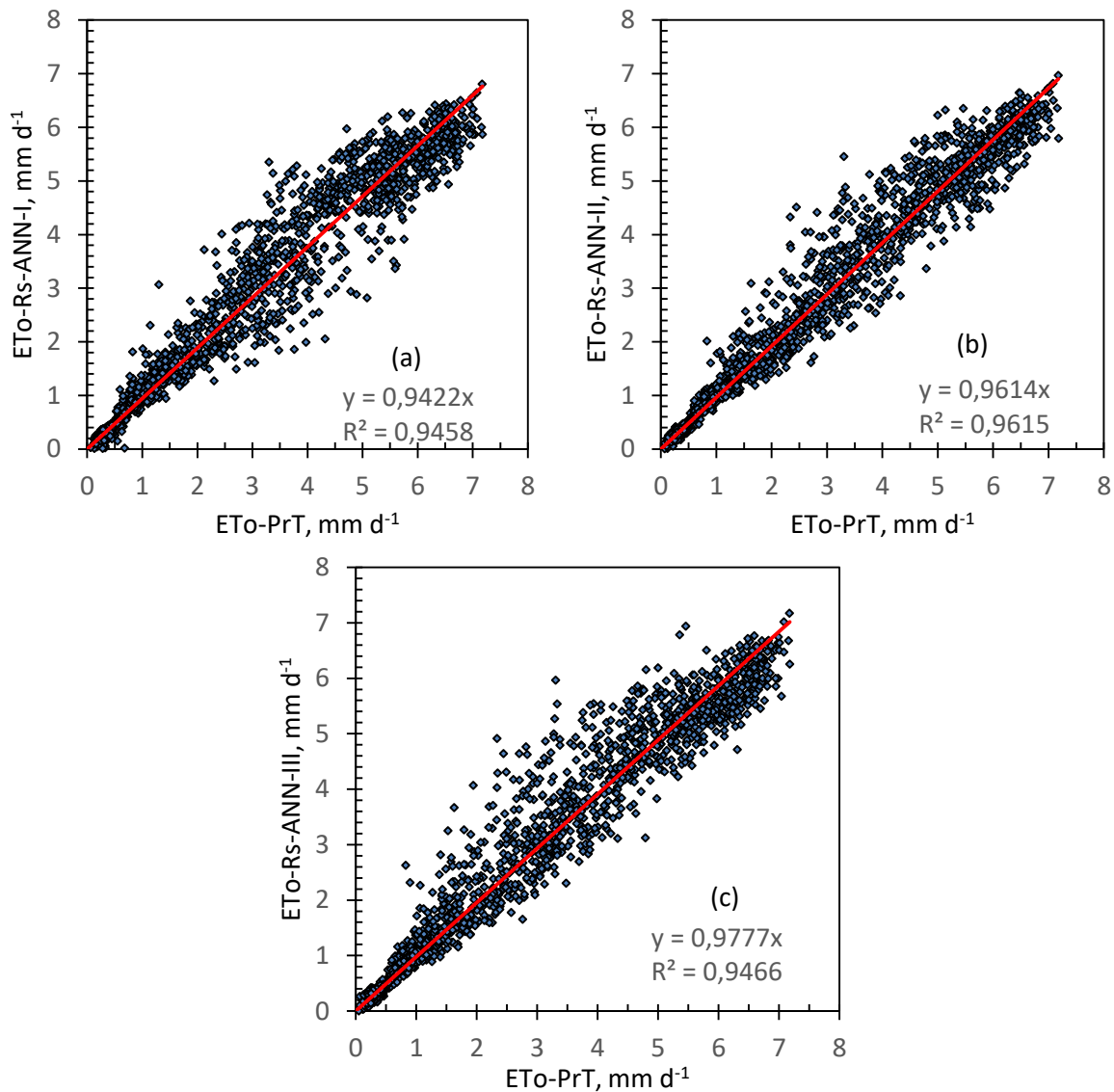


346

347

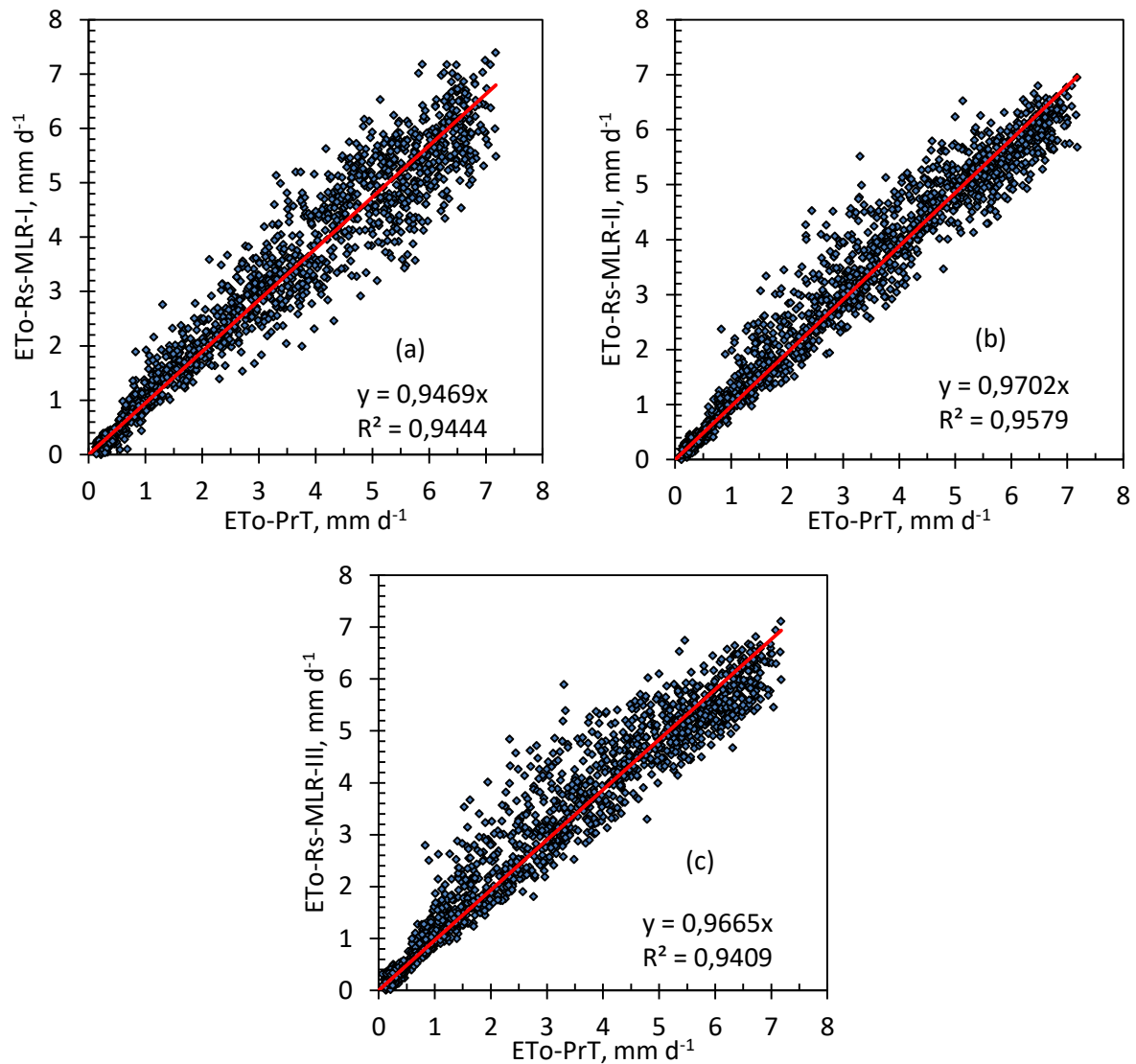
348 *Figure 8. Scattering diagrams between ET_o -PM estimated with R_s measured and ET_o -PM estimated with*
 349 *R_s computed with multi-linear regression (a. MLR-I, b. MLR-II and c. MLR-III) models at Amyntaio*
 350 *station.*
 351

352 Figures 9 and 10 present the comparison between ET_o of Priestley-Taylor method estimated
 353 using R_s measurements and ET_o estimated with R_s computed with a) Artificial Neural Networks
 354 (ANNs) and b) multilinear regression (MLR) models at Amyntaio Station.



356 *Figure 9. Scattering diagrams between ET_o -PrT estimated with R_s measured and ET_o -PrT estimated with*
 357 *R_s computed with Artificial Neural Networks (a. ANN-I, b. ANN-II and c. ANN-III) models at Amyntaio*
 358 *station.*
 359
 360

361 The values of R^2 are very high in these three scatters diagrams (0.946 to 0.962).
 362 Underestimation of higher values of ET_o -PrT observed, with lower using the ANN-I model.



363

364

365 *Figure 10. Scattering diagrams between ET₀-PrT estimated with R_s measured and ET₀-PrT estimated*
 366 *with R_s computed with multi-linear regression (a. MLR-I, b. MLR-II and c. MLR-III) models at Amyntaio*
 367 *station.*

368

369 The values of R² are very high in these three scatters diagrams (0.941 to 0.958).
 370 Underestimation of higher values of ET₀-PrT is also observed, with lower values when the MLR-
 371 I model is used.

372 The statistical criteria of models to estimate the ET₀ at Amyntaio meteorological station
 373 using the R_s values estimated using the Hargreaves. ANNs and MLRs models are presented in
 374 Table 5.

375 The correlation coefficient for the Hargreaves method for ET₀ is 0.986 for the original
 376 equation and 0.937 for the local adjusted equation.

377 The values of r for ANNs and MLR models ranged from 0.983 to 0.988 for ET₀-PM
 378 method, while for ET₀-PrT method it ranged from 0.973 to 0.981 and 0.972 to 0.980, respectively

379 for ANNs and MLR models. The ET_o values computed using the MLR-II and ANN-II models
 380 show high accuracy in correlation with the values of ET_o estimated using measured R_s . In general,
 381 the ET_o estimated using the ANN and MLR models, as well as the Hargreaves method,
 382 demonstrate high accuracy (with r ranging from 0.937 to 0.988).

383 The scattering diagrams, the comparison between the estimated values of ET_o with the
 384 Penman-Monteith method and the statistical criteria show that the three methods describe with
 385 high accuracy the ET_o at Amyntaio station.

386

387

Table 5.

388

Statistical criteria of Hargreaves, ANNs and MLR models to estimate ET_o at AMYNTAIO station

	ET_o -PM				ET_o -PrT			
	Ave mm d ⁻¹	r	RMSE mm d ⁻¹	EF	Ave mm d ⁻¹	r	RMSE mm d ⁻¹	EF
ET_o -PM	2.806							
ANN-I	2.724	0.983	0.373	0.964	2.69	0.973	0.516	0.936
ANN-II	2.788	0.988	0.313	0.975	2.73	0.981	0.429	0.957
ANN-III	2.805	0.985	0.343	0.970	2.80	0.974	0.490	0.945
MLR-I	2.736	0.983	0.371	0.965	2.70	0.972	0.519	0.936
MLR-II	2.788	0.988	0.313	0.975	2.78	0.980	0.436	0.955
MLR-III	2.800	0.985	0.355	0.968	2.80	0.972	0.436	0.954
HG	2.687	0.986	0.385	0.962				
HG Local	3.032	0.937	0.744	0.858				

389

390 4. DISCUSSION

391

392 The accurate estimation of ET_o is very interesting in agriculture, engineering, hydrology,
 393 ecology and decision makers. It requires measurements of many meteorological parameters, in
 394 which the more significant is the solar radiation. It is a meteorological variable which in many
 395 stations are not measured or when it measured it is of low accuracy. The reasons are the cost,
 396 maintenance and calibration requirements of the measuring equipment (Despotovic et al., 2015).
 397 In the Greek territory, many meteorological stations have been established in the last decades
 398 (National Observatory of Athens/Meteo.gr). In most of them, solar radiation is not measured. In
 399 the cases of lack of solar measurements, the indirect estimation of R_s is necessary to estimate
 400 ET_o . The machine learning models are the alternative methods that used more recently.

401 The developed in this work, empirical equations such as Hargreaves, ANNs and MLR
 402 models to estimate R_s using available datasets from our study areas in the Northern Greece region
 403 showed that they have the ability to describe it with high accuracy. The models of ANNs and
 404 MLR methods that derived using different combination of input variables were evaluated. In

405 these combination the following variables were used: T_{\max} , T_{\min} , T_{ave} , RH_{av} , u_2 in the 1st, R_a , (T_{\max} -
 406 T_{\min}), (T_{\max} - T_{\min})^{0.5}, RH_{av} in the 2nd and R_a , and (T_{\max} - T_{\min})^{0.5} in 3rd.

407 The extraterrestrial radiation (R_a) could improve the accuracy of estimations, either using
 408 ANN models or MLR methods. The R_a is incorporated in the Hargreaves equation. Using the R_a
 409 and the factor of (T_{\max} - T_{\min})^{0.5}, as input better performance was observed.

410

411 **4.1 Evaluation of R_s models**

412 The derived ANN models can reasonably estimate the daily radiation, The coefficient of
 413 determination (r) ranged from 0.861 to 0.936, the RMSE ranged from 3.271 to 4.451 MJ m⁻² d⁻¹
 414 and the EF ranged from 0.652 to 0.848, respectively, using the data from the two stations. The
 415 results of this work align with the conclusions drawn by Zhang et al. (2017). They concluded that
 416 the ANNs models can reasonably estimate the daily radiation, with RMSE values in the range of
 417 1.24–4.2 MJ m⁻²d⁻¹ for daily radiation. However it is unclear, whether the improvement in
 418 accuracy of ANNs models, when compared to empirical models, is significant.

419 The statistical criteria for the derived MLR models show that the values of r ranged from
 420 0.871 to 0.929, RMSE ranged from 3.408 to 4.210 MJ m⁻² d⁻¹ and EF ranged from 0.681 to
 421 0.840, respectively, using the data from the two stations.

422 The r , RMSE and EF of Hargreaves method for R_s was 0.893 and 0.908, 3.049 and 4.197
 423 MJ m⁻²d⁻¹ and 0.732 and 0.688, respectively for each station AUTH and AMIN, when K_{RS} =0.162.
 424 The accuracy of R_s estimation showed a slight improvement when K_{RS} =0.178 was used.

425 Using five years of daily data sets, in the present analysis, to derive the R_s models of
 426 Hargreaves, ANNs and MLR methods, and comparing them to three years of daily data
 427 (Antonopoulos et al. 2019), result in minor changes in the statistical criteria for the same modules
 428 of ANNs or MLR models. The percentile changes in r ranged from 1.51 to -5.44 % at the AUTH
 429 station and from -0.11 to 0.54 % at the Amyntaio station. The changes in RMSE and EF are more
 430 significant for the AUTH station data (average 11.61 and -3.17 %) compared to the AMIN station
 431 data (average -0.37 and 1.41 %).

432 Despotovic et al. (2015) concluded that the different R_s models, even though they might
 433 have better performance with the data used for model development that cannot be recommended
 434 for global use. Aladenola, and Madramootoo (2014) presented an evaluation of suitability of nine
 435 models to estimate R_s , and their effect on ET_o calculated with FAO-56 PM. The estimated R_s
 436 when compared with the measured R_s , did not show significant differences. The authors
 437 suggested that in Canada, the Samani and Hargreaves-Samani models (1982; 1985) are
 438 recommended for estimating R_s . The conclusion of Zhang et al. (2017), on the non-sunshine

439 duration empirical models which include the difference between maximum and minimum
 440 temperature, relative humidity, cloud cover, precipitation, and vapor pressure, summarized that
 441 the RMSE values of those models ranged from 2.05 to 4.70 MJ m⁻²d⁻¹. Zang et al. (2022)
 442 summarized that the various empirical models combining different meteorological parameters to
 443 estimate R_s , perform well only in areas where the required meteorological data are available. A
 444 comprehensive analysis of the related literature reveals that an issue exists where empirical
 445 models are site-dependent, and empirical models trained at one site may not be suitable for
 446 another site with a different climate. In a study of six different machine-learning algorithms to
 447 predict daily solar radiation at 27 European countries. Nematchoua et al. (2022) concluded that
 448 for all the algorithms, the r^2 values range from 0.382 to 0.985, while the RMSE values ranged
 449 from 0.145 to 2.126 MJ m⁻² d⁻¹.

450

451 *Table 6. Changes of average, sd, r, RMSE and EF of R_s at AUTH and AMIN stations when using 3 and 5*
 452 *years daily sets of data.*

AUTH	Average R_s , %	sd of R_s , %	R, %	RMSE, %	EF, %
Ave	6.12	0.60	-2.16	11.61	-3.17
max	13.00	5.68	1.51	26.11	5.92
min	2.95	-1.62	-5.44	-9.55	-9.86
AMYNTAIO					
Ave	2.96	2.69	0.27	-0.37	1.41
max	5.80	6.81	0.54	1.36	3.30
min	1.07	1.36	-0.11	-3.30	0.00

453

454 Nawab et al. (2023) concluded that Artificial Intelligent (AI) methods are more accurate
 455 than empirical methods and that the modified sunshine-based models were more accurate
 456 compared to empirical methods. Moreover, the artificial neural networks and Hybrid models had
 457 the highest accuracy amongst the AI methods.

458

459 **4.2 Evaluation of ET_o methods**

460 Two of most important methods of ET_o estimation were evaluated in this work. Both of
 461 them, the Penman-Monteith and the Priestley-Taylor methods, are based on the combination of
 462 radiation and temperature.

463 The values of r , RMSE and EF for ET_o calculation using the Hargreaves method in relation
 464 to ET_o -PM with R_s measured are 0.932, 0.889 mm d⁻¹ and 0.712, for the AUTH station and 0.986,
 465 0.385 mm d⁻¹ and 0.962, for the AMIN station, respectively.

466 The results of the present work to calculate ET_o using the FAO-56 PM equation, while
 467 using the derived R_s from the models in this study, indicate an acceptable level of accuracy.

468 The values of r , RMSE and EF for ET_o calculation obtained using the derived ANNs
469 models ranged from 0.963 to 0.978, 0.314 to 0.410 mm d⁻¹ and 0.917 to 0.952, respectively, for
470 the AUTH station. Similarly, for the AMIN station, the values ranged from 0.983 to 0.988, 0.313
471 to 0.373 mm d⁻¹ and 0.964 to 0.975, respectively.

472 The statistical criteria obtained by the comparison of ET_o -PM using MLR models and ET_o -
473 PM using measured R_s showed consistency, with values for r , RMSE and EF ranging from 0.983
474 to 0.988, 0.313 to 0.371 mm d⁻¹ and 0.965 to 0.975, respectively for the AUTH station. While
475 for the AMIN station, these values ranged from 0.983 to 0.986, 0.313 to 0.371 mm d⁻¹ and 0.965
476 to 0.975, respectively.

477 The results of present work to calculate ET_o using the Priestley-Taylor method, while using
478 the derived R_s from the models in this study, indicate also an acceptable level of accuracy.

479 The values of r , RMSE and EF for ET_o -PrT calculation using the derived ANN models
480 comparing with ET_o -PrT calculation using measured values of R_s ranged from 0.973 to 0.991,
481 0.429 to 0.626 mm d⁻¹ and 0.936 to 0.982, respectively, for the two stations. The ANN-II model
482 show better values of statistical criteria and the ANN-I the worse values.

483 The statistical criteria obtained by the comparison of ET_o -PrT using MLR models and ET_o -
484 PrT using measured R_s showed accuracy, with values for r , RMSE and EF ranging from 0.972 to
485 0.990, 0.436 to 0.556 mm d⁻¹ and 0.936 to 0.974, respectively for the two stations. The better
486 values of statistical criteria are showed by the ANN-II model and the worse values of MLR-I.

487 Similar results have been observed in other studies using ANNs models by different
488 authors, as presented by Terzi and Keskin (2010), Diamantopoulou et al. (2011), Gocic et al.
489 (2016), Shiri et al. (2014). The comparison results of Antonopoulos and Antonopoulos (2017)
490 found that ANNs models, as well as empirical equations, estimated ET_o with accuracy.
491 Specifically, the RMSE ranged from 0.574 to 1.33 mm d⁻¹, and r ranged from 0.955 to 0.986
492 when using daily data from the Amyntaio station and measured R_s values. These findings align
493 with the results and conclusions of many other authors that examined empirical equations for
494 ET_o estimations (Xu and Singh, 2002; Lu et al., 2005; Xystrakis and Matzarakis, 2011; Rácz, et
495 al. 2013; Efthimiou et al. 2013; Bogawski et al. 2014; Heydari et al. 2014; Tigkas et al. 2020).

496 Aladenola and Madramootoo (2014) examined the effects of nine models to estimate R_s on
497 the ET_o computed with FAO-56 PM. They concluded that the effects was highly reduced in
498 calculated ET_o . In the study of Bellido-Jimenez et al. (2022) of ET_o using a regional machine
499 learning method in Southern Spain got statistical values of RMSE and r^2 of 0.657 to 0.703 mm
500 d⁻¹ and 0.897 to 0.931, respectively.

501 The results of the evaluation of the empirical Hargreaves method, multi-linear regression
502 models, and artificial neural networks models using measured solar radiation values showed that
503 these models can effectively be used to estimate solar radiation at stations without direct
504 measurements. When these different models are used to estimate solar radiation and then ET_o ,
505 with the Penman-Monteith and Priestley-Taylor methods, at nearby stations where solar radiation
506 is not being measured, similar results are obtained. These findings suggest that this procedure
507 can be reliably used to estimate ET_o in such situations.

508

509 **5. Conclusions**

510

511 The reference evapotranspiration (ET_o) with the Penman-Monteith and Priestley-Taylor
512 methods estimated using indirect methods to calculate solar radiation (R_s) was evaluated. These
513 indirect methods include the Hargreaves method, models based on ANN technology and models
514 using MLR method. Daily meteorological data from two stations in northern Greece were utilized
515 for the development of solar radiation models and ET_o estimation,

516 Three different ANNs and MLR models were derived, each using a different number and
517 type of input or independent variables.

518 The scattering diagrams comparing the estimated and measured values of R_s , along with
519 the statistical criteria, indicate that the indirect model accurately describes R_s at the two
520 meteorological stations. The r and EF values of statistical indexes ranged from 0.860 to 0.871
521 and 0.650 to 0.681, respectively, while the RMSE values ranged from 4.21 to 4.751 $MJ\ m^{-2}d^{-1}$.
522 The RMSE values indicated similarity to those reported in other models describing R_s as
523 summarized by Zang et al. (2017). The inclusion of R_a and the factor of $(T_{max}-T_{min})^{1/2}$ in the
524 ANNs and MLR models improved the accuracy of the results. The results of ANNs models, when
525 compared to MLR models using the same input variables, are consistent between them.

526 The values obtained from ET_o -PM and ET_o -PrT methods, when R_s is indirectly estimated
527 using ANNs and MLR, models, show high accuracy in ET_o estimation. The statistics of ET_o
528 estimation at the two stations for both ET_o methods, showed that the r and EF values, between
529 ET_o estimated using the indirect R_s models and ET_o estimated using R_s measured, were greater
530 than 0.963 and 0.918, respectively, while the RMSE values were lower than 0.646 $mm\ d^{-1}$. The
531 ET_o -PM using MLR models of R_s estimation showed better accuracy ($r>0.983$, $EF>0.964$ and
532 $RMSE<0.37\ mm\ d^{-1}$) compared to ANNs models of R_s estimation ($r>0.963$, $EF>0.917$ and
533 $RMSE<0.41\ mm\ d^{-1}$). The ET_o -PrT produced similar results of statistical indexes using either
534 MLR or ANNs models of R_s estimation. The inclusion of R_a , the factor $(T_{max}-T_{min})^{1/2}$ and relative

535 humidity as input variables in MLR models resulted in higher accuracy. The ANN model with
536 the same input variables and parameters followed in accuracy.

537 The R_s and ET_o of the Hargreaves method were also evaluated in comparison to the
538 measured R_s and ET_o of Penman-Monteith method. The result showed high accuracy, with high
539 values of statistical indexes (r and EF greater than 0.893 and 0.722, respectively, and RMSE
540 lower than $3.86 \text{ MJ m}^{-2}\text{d}^{-1}$ for R_s , and r and EF greater than 0.932 and 0.826, respectively, and
541 RMSE lower than 0.744 mm d^{-1} for ET_o).

542 Empirical methods for estimating solar radiation, which can subsequently be used to
543 estimate reference evapotranspiration continue to be valuable tools, and remain highly interesting
544 in hydrological and agronomical studies. They provide one of the main components of
545 hydrological balance. The accuracy of reference evapotranspiration with the Penman-Monteith
546 and Priestley-Taylor methods is within an acceptable range when these empirical methods were
547 used as input data in the absence of radiation measurements. The multi-linear regression models
548 are highly accurate and are on par with artificial neural networks. However, achieving accurate
549 results with these methods requires special knowledge from the users and a significant dataset
550 with the same variables used to estimate ET_o .

551

552

556 **References**

- 557 Aladenola, O.O., Madramootoo, C. A., 2014. Evaluation of solar radiation estimation methods for
558 reference evapotranspiration estimation in Canada. *Theoretical and Applied Climatology*,
559 118(3):377-385.
- 560 Alexandris, S., Kerkides, P., Liakatas, A., 2006. Daily reference evapotranspiration estimates by the
561 Copais approach, *Agric. Water Manag.*, 82, 371-386.
- 562 Allen, R.G., Pruitt, W.O., 1991. FAO-24 reference evapotranspiration factors. *J. of Irrig. and Drain.Eng.*,
563 ASCE, 117, 758-773.
- 564 Allen, R.G., Pereira, L.S., Raes, D., Smith, M., 1998. Crop evapotranspiration-guidelines for computing
565 crop water requirements, FAO Irrigation and Drainage. Paper 56, Rome, Italy.
- 566 Ampas, V., Baltas, E., Papamichail, D., 2007. Comparison of Different Methods for the Estimation of the
567 Reference Crop Evapotranspiration in the Florina Region, *WSEAS Trans, Environ. Development*,
568 12(2), 1449-1454.
- 569 Antonopoulos, V. Z., Gianniou, S.K., 2003. Simulation of water temperature and dissolved oxygen
570 distribution in Lake Vegoritis, Greece. *Ecol. Model.*, 160, 39-53.
- 571 Antonopoulos, V.Z., Antonopoulos, A.V., 2017. Daily reference evapotranspiration estimates by artificial
572 neural networks technique and empirical equations using limited input climate variables. *Comput.*
573 *Electron. Agric.*, 132. 86 - 96 ,

- 574 Antonopoulos, V.Z., Gianniou, S.K., Antonopoulos, A.V., 2016. Artificial neural networks and empirical
575 equations to estimate daily evaporation: application to lake Vegoritis, Greece. *Hydrol. Sci. J.* 61. 2590-
576 2599.
- 577 Antonopoulos, V.Z., Papamichail, D.M., Aschonitis, V.G., Antonopoulos, A.V., 2019. Solar radiation
578 estimation methods using ANN and empirical models. *Comput. Electron. Agric.*, 160, 160 - 167 .
- 579 Aschonitis, V.G., Antonopoulos, V.Z., Papamichail, D.M., 2012. Evaluation of pan coefficient equations
580 in a semi-arid Mediterranean environment using the ASCE standardized Penman-Monteith method.
581 *Agr. Sci.* 3(1). 58-65.
- 582 Aschonitis, V.G., Demertzi, K., Papamichail, D.M., Colombani, N., Mastrociccio, M., 2015. Revisiting
583 the Priestley-Taylor method for the assessment of reference crop evapotranspiration in Italy, *Italian J.*
584 *Agrometeorology.* 20 (2). 5-18.
- 585 Aschonitis, V.G., Papamichail, D., Demertzi, K., Colombani, N., Mastrociccio, M., Ghirardini, A.,
586 Castaldelli, G., Fano, E.-A., 2017. High-resolution global grids of revised Priestley-Taylor and
587 Hargreaves-Samani coefficients for assessing ASCE-standardized reference crop evapotranspiration
588 and solar radiation. *Earth System Science Data* 9(2), 615-638.
- 589 Bellido-Jimenez, A., Estevez, J., García-Marín, A.P., 2022. A regional machine learning method to
590 outperform temperature-based reference evapotranspiration estimations in Southern Spain. *Agric.*
591 *Water Manag.*, 274, 107955.
- 592 Besharat, F., Dehghan, A. A. Faghih, A.R., 2013. Empirical models for estimating global solar radiation:
593 A review and case study. *Renewable and Sustainable Energy Reviews* 21 (2013) 798–821
- 594 Bogawski, P., Bednorz, E., 2014. Comparison and validation of selected evapotranspiration models for
595 conditions in Poland (Central Europe). *Water Resour. Manage.* 28. 5021 –5038. DOI 10.1007/s11269-
596 014-0787-8
- 597 Daut, I., Irwanto, M., Irwan, Y.M., Gomesh, N., Ahmad, N.S., 2011. Combination of Hargreaves method
598 and linear regression as a new method to estimate solar radiation in Perlis, Northern Malaysia. *Solar*
599 *Energy* 85 (11), 2871–2880.
- 600 Despotovic, M., Nedica, V., Despotovic, D., Cvetanovic, S., 2015. Review and statistical analysis of
601 different global solar radiation sunshine models. *Renewable and Sustainable Energy Reviews* 52:
602 1869–1880.
- 603 Diamantopoulou, M.L., Georgiou, P.E., Papamichail, D.M., 2011. Performance evaluation of artificial
604 neural networks in estimation references evapotranspiration with minimal meteorological data. *Global*
605 *Nest J.* 13. 18-27.
- 606 Djaman, K., Baldea, A.B., Sow, A., Mullera, B., Irmak, S., N'Diaye, M.K., Manneha, B., Moukoumbia,
607 Y. D., Futakuchic, K., Saitoc, K., 2015. Evaluation of sixteen reference evapotranspiration methods
608 under sahelian conditions in the Senegal River Valley. *J. Hydrol.: Regional Studies*, 139–159
- 609 Efthimiou, N., Alexandris, S., Karavitis, C., Mamassis, N., 2013. Comparative analysis of reference
610 evapotranspiration estimation between various methods and the FAO56 Penman - Monteith
611 procedure, *European Water*, 42: 19-34.
- 612 El-Sebaili, A.A., Al-Hazmi, F.S., Al-Ghamdi, A.A., Yaghmour, S.J., 2010. Global, direct and diffuse solar
613 radiation on horizontal and tilted surfaces in Jeddah, Saudi Arabia. *Applied Energy* 87 (2), 568–576.
- 614 Gianniou, S. K., Antonopoulos, V.Z., 2007. Evaporation and energy budget in Lake Vegoritis, Greece. *J.*
615 *Hydrol.* 345. 212-223.
- 616 Jain, S.K., Nayak, P.C., Sudheer, K.P., 2008. Models for estimating evapotranspiration using artificial
617 neural networks and their physical interpretation. *Hydrol. Process.* 22. 2225–2234.
- 618 Hargreaves, G.H., 1994. Simplified coefficients for estimating monthly solar radiation in North America
619 and Europe. Departmental Paper, Dept. of Biol. and Irrig. Engrg., Utah State University, Logan, Utah.
- 620 Hargreaves, G.H., Samani, Z.A., 1985. Reference crop evapotranspiration from temperature. *Trans.*
621 *ASAE* 1(2). 96-99.
- 622 Hargreaves, G.H., Samani, Z.A., 1982. Estimating potential evapotranspiration. *J. Irrig. Drain. Eng.*
623 *ASCE* 108 (3). 225–230.
- 624 Heddum, S., 2014. Modelling hourly dissolved oxygen concentration (DO) using dynamic evolving
625 neural- fuzzy inference system (DENFIS)-based approach: case study of Klamath River at Miller
626 Island Boat Ramp. OR. USA. *Environ. Sci. Pollut. Res.* 21:9212–9227

- 627 Heydari, M.M., Aghamajidi, R., Beygipoor, G., Heydari, M., 2014. Comparison and evaluation of 38
628 equations for estimating reference evapotranspiration in an arid region, *Fresenius Environ. Bulletin*,
629 23, 1985-1997.
- 630 Kisi, O., Sanikhani, H., Zounemat-Kermani, M., Niazi, F., 2015. Long-term monthly evapotranspiration
631 modeling by several data-driven methods without climatic data. *Comput. Electron. Agric.* 115. 66-77.
632 ISSN 0168-1699.
- 633 Kumar, M., Raghuvanshi, N.S., Singh, R., 2011. Artificial neural networks approach in
634 evapotranspiration modeling: a review, *Irrig. Sci.*, 29:11–25
- 635 Laaboudi, A., Mouhouche, M., Draoui, B., 2012. Neural network approach to reference
636 evapotranspiration modeling from limited climatic data in arid regions. *Int. J. Biometeorol.* 56. 831–
637 841
- 638 Li, H., Ma, W., Lian, Y., Wang, X., Zhao, L., 2011. Global solar radiation estimation with sunshine
639 duration in Tibet, China. *Renewable Energy* 36 (11), 3141-3145.
- 640 Lu, J., Sun, G., McNulty, S.G., Amatya, D.M., 2005. A comparison of six potential evapotranspiration
641 methods for regional use in the southeastern United States. *J. Amer. Water Resour. Assoc. (JAWRA)*,
642 621-633.
- 643 Nawab, F., Abd Hamid, A.S., Ibrahim, A., Sopian, K., Fazlizan, A., Fauzan, M.F., 2023. Solar irradiation
644 prediction using empirical and artificial intelligence methods: A comparative review. *Heliyon* 9,
645 e17038.
- 646 Nematchoua, M.K., Orosa J.A., Afafia, M., 2022. Prediction of daily global solar radiation and air
647 temperature using six machine learning algorithms; a case of 27 European countries. *Ecological*
648 *Informatics*, 69, 101643.
- 649 Premalatha, N., Valan Arasu, A., 2016. Prediction of solar radiation for solar systems by using ANN
650 models with different back propagation algorithms. *J. of Applied Research and Technology*, 14:206-
651 214.
- 652 Priestley, C., Taylor, R., 1972, On the assessment of surface heat flux and evaporation using large-scale
653 parameters. *Monthly Weather Rev.* 100 (2). 81-92.
- 654 Rácz, C., Nagy, J. Dobos, A.C., 2013. Comparison of Several Methods for Calculation of Reference
655 Evapotranspiration, *Acta Silv. Lign. Hung.* 9.
- 656 Raziqi, T, Pereira, L.S., 2013. Estimation of ETo with Hargreaves-Samani and FAO-PM temperature
657 methods for a wide range of climate in Iran. *Agricultural Water Management*, 121: 1– 18
- 658 Rivero, M., Orozco, S., Sellschopp, F.S., Loera-Palomo, R., 2017. A new methodology to extend the
659 validity of the Hargreaves-Samani model to estimate global solar radiation in different climates: Case
660 study Mexico. *Renewable Energy* 114, 1340–1352.
- 661 Shiri, J., Nazemi, A.H., Sadraddini, A.A., Landaras, G., Kisi, O., Fard, A.F., Marti, P., 2014. Comparison
662 of heuristic and empirical approaches for estimating reference evapotranspiration from limited inputs
663 in Iran. *Comput. Electron. Agric.* 108. 230-241.
- 664 Su, Q., Singh, V.P., Karthikeyan, R., 2022. Improved reference evapotranspiration methods for regional
665 irrigation water demand estimation. *Agric. Water Manag.*, 274: 107979
- 666 Terzi, O., Keskin, M.E., 2010. Comparison of artificial neural networks and empirical equations to
667 estimate daily pan evaporation. *Irrig. Drain.* 59. 215–225.
- 668 Tigkas, D., Vangelis, H. & Tsakiris, G., 2020. Implementing Crop Evapotranspiration in RDI for Farm-Level
669 Drought Evaluation and Adaptation under Climate Change Conditions. *Water Resour Manage* 34, 4329–
670 4343. <https://doi.org/10.1007/s11269-020-02593-6>
- 671 Xystrakis, F., Matzarakis, A., 2011. Evaluation of 13 Empirical Reference Potential Evapotranspiration
672 Equations on the Island of Crete in Southern Greece. *J. Irrig. Drain Eng.*, 2011, 137(4): 211-222
- 673 Xu, C.-Y., Singh, V.P., 2000. Evaluation and Generalization of Radiation-based Methods for Calculating
674 Evaporation, *Hydrol. Processes* 14, 339–349.
- 675 Xu, C.-Y., Singh, V.P., 2002. Cross Comparison of Empirical Equations for Calculating Potential
676 Evapotranspiration with Data from Switzerland. *Water Resour. Manag.*, 16: 197–219

- 677 Utset, A., Farré, I., Martínez-Cob, A., Cavero, J., 2004. Comparing Penman-Monteith and Priestley-
678 Taylor approaches as reference evapotranspiration, Inputs for modeling maize water-use under
679 Mediterranean conditions. *Agric. Water Manage.*, 66, 205-219
- 680 Valiantzas, J.D., 2018. Modification of the Hargreaves-Samani model for estimating solar radiation from
681 temperature and humidity data. *J. Irrig. Drain. Eng.*, ASCE, 144:06017014.
- 682 Yadav, A.K., Chandel, S.S., 2014. Solar radiation prediction using Artificial Neural Network techniques:
683 A review *Renewable and Sustainable Energy Reviews* 33 : 772–781
- 684 Yao, H., 2009. Long-term study of lake evaporation and evaluation of seven estimation methods: Results
685 from Dickie Lake. south-central Ontario. Canada. *J. Water Resour. Prote.* 2. 59-77.
- 686 Zang, H., Jiang, X., Cheng, L., Zhang, F., Wei, Z., Sun, G., 2022. Combined empirical and machine
687 learning modeling method for estimation of daily global solar radiation for general meteorological
688 observation stations. *Renewable Energy* 195, 795-808.
- 689 Zhang, J., Zhao, L., Deng, S., Xu, W., Zhang, Y., 2017. A critical review of the models used to estimate
690 solar radiation. *Renewable and Sustainable Energy Reviews* 70 : 314–329.
- 691
- 692
- 693